Volume 19, Number 3, 2026. pp. 303-311

Jordan Journal of Physics

ARTICLE

Dynamics of a Quasi-One-Dimensional Quantum Droplet in Harmonic Potential

Nor A. B. Aklan[a], **Bakhtiyor Baizakov**[b,c], **Anis S. Samiun**[a] and **Bakhram Umarov**[b]

[a] *Department of Computational and Theoretical Sciences, Kulliyyah of Science, International Islamic University of Malaysia, 25200 Kuantan, Pahang.*

[b] *Physical-Technical Institute, Uzbek Academy of Sciences, 100084, Tashkent, Uzbekistan.*

[c] *Institute of Theoretical Physics, National University of Uzbekistan,100174, Tashkent, Uzbekistan.*

Doi: **https://doi.org/10.47011/19.3.2**

Received on: 15/01/2025; *Accepted on: 04/11/2025*

Abstract: The dynamics of a quasi-one-dimensional quantum droplet (QD) confined to a harmonic potential were investigated. A variational approach using a super-Gaussian trial function was developed to estimate the QD parameters. The predictions of the variational analysis were compared with numerical simulations of the governing Gross-Pitaevskii equation, revealing a strong qualitative agreement. The liquid-like behaviour of flat-top QDs performing dipole oscillations in the harmonic trap was demonstrated numerically. When an additional potential barrier was introduced at the center of the harmonic trap, the incoming QD exhibited a peculiar reflection, resembling that of a slowly moving liquid droplet bouncing off a non-wetted wall. Interference phenomena, typically associated with the reflection of wave packets from potential barriers, appeared to be suppressed for QDs.

Keywords: Gross-Pitaevskii equation, Harmonic potential, Nonlinear equations, Quantum droplet, Variational approximation method.

PACs: 03.75.Kk; 03.75.Mn; 03.75.Lm; 03.75.Hh.

1. Introduction

Theoretical predictions and experimental observations of a new state of matter, known as a quantum droplet (QD), initiated active research to understand its properties [1–3]. Although the existence of QDs was initially predicted for two-component Bose gas mixtures, the first experimental realization occurred in single-component Bose-Einstein condensates (BEC) with dipolar atomic interactions, later expanding to binary Bose gas mixtures [4–8]. The emergence of QDs depends on a delicate balance between mean-field atomic interactions in the mixture condensate and the effects of quantum fluctuations, first elaborated by Lee, Huang and Yang [9]. Under normal conditions, the quantum correction term in the Bose gas ground-state energy, described by the LHY term, is negligibly small compared to the contribution of other terms in the governing Gross-Pitaevskii equation (GPE). However, when intra-component repulsion in binary condensate mixtures is nearly balanced by inter-component attraction, the contribution of the LHY term becomes significant, stabilizing the mixture and enabling the existence of a self-trapped state with unique properties. In three-dimensional (3D) and two-dimensional (2D) free space, the mixture condensate would collapse without the stabilizing effect of repulsive quantum fluctuations. In contrast, in a quasi-1D setting with extremely tight radial confinement, the quantum fluctuation term can be attractive for both BECs with contact [10] and dipolar [11] interactions. Self-trapped localized states, known

Corresponding Author: Nor Amirah Busul Aklan **Email**: noramirah@iium.edu.my

as *one-dimensional quantum droplets*, emerge from competing nonlinearities (attractive quadratic and repulsive cubic) [12, 13].

The atomic density of quantum droplets ($n_{QD}\sim10^{15}\text{cm}^{-3}$ [8]) is higher than the typical density of gaseous BEC ($n_{BEC}\sim10^{13}-10^{14}\text{cm}^{-3}$ [14]), but much smaller than the atomic/molecular density of ordinary liquids such as water ($n_{Liq}\sim10^{22}\text{cm}^{-3}$). The most interesting property of quantum droplets is that, despite being extremely dilute compared to normal liquids, QDs display incompressibility and surface tension [15], which are inherent to typical liquids. The unique properties of these exotic quantum states of matter continue to make them an interesting subject of investigation. In theoretical studies, the governing GPE for QD dynamics generally does not admit analytic solutions in settings such as the presence of an external potential. In this situation, approximate analytical methods, such as the variational approach and perturbation theory, can be useful. The variational approach for one-dimensional QDs in free space has been explored extensively [13, 16]. However, under real experimental conditions, condensates are always held within external potentials, and essential information is retrieved by manipulating the trap parameters or internal parameters of the condensate, making it essential to consider these effects in theoretical models. The effect of the harmonic trap on the dynamics of a two-dimensional rotating QD has been reported in a recent article [17].

The objective of this study is to explore the static and dynamic properties of quantum droplets confined to a harmonic potential, emphasizing their liquid-like behavior. To this end, in the following sections, we develop a variational approach for analytical treatment and perform systematic numerical simulations of the governing GPE to unveil specific features of QDs.

2. The Model and Governing Equations

The dynamics of a quasi-1D binary BEC in the presence of the quantum fluctuations term and an external potential is described by the coupled GPEs [12, 18]:

$$\begin{aligned} i\hbar\partial_t\psi_1 &= -\frac{\hbar^2}{2m}\partial_x^2\psi_1 - V(x)\psi_1 \\ &+ G_1|\psi_1|^2\psi_1 - G_{12}|\psi_2|^2\psi_1 \\ &- \frac{g_1 m^{1/2}}{\pi\hbar}\sqrt{g_1|\psi_1|^2+g_2|\psi_2|^2}\psi_1, \end{aligned} \tag{1}$$

$$\begin{aligned} i\hbar\partial_t\psi_2 &= -\frac{\hbar^2}{2m}\partial_x^2\psi_2 - V(x)\psi_2 \\ &+ G_2|\psi_2|^2\psi_2 - G_{12}|\psi_1|^2\psi_2 \\ &- \frac{g_2 m^{1/2}}{\pi\hbar}\sqrt{g_1|\psi_1|^2+g_2|\psi_2|^2}\psi_2, \end{aligned} \tag{2}$$

where $\psi_1(x,t)$, $\psi_2(x,t)$ are the mean-field wave functions of the binary condensate, $V(x)$ is the external trapping potential, g_1 and g_2 are the intra- and g_{12} are the inter-component coupling coefficients, and *m* is the atomic mass (supposed to be equal for both components). The indices denote corresponding derivatives $\partial_t=\partial/\partial t$, $\partial_x^2=\partial^2/\partial x^2$. The auxiliary coefficients below are introduced to simplify the equations

$$G_1 = g_1 + \frac{2g_2\left(g_1g_2+g_{12}\sqrt{g_1g_2}\right)}{(g_1+g_2)^2},$$

$$G_2 = g_2 + \frac{2g_1\left(g_1g_2+g_{12}\sqrt{g_1g_2}\right)}{(g_1+g_2)^2},$$

$$G_{12} = \frac{\sqrt{g_1g_2}(g_1^2+g_2^2-2g_{12}\sqrt{g_1g_2})}{(g_1+g_2)^2}.$$

For the analytical treatment and numerical simulations, it is convenient to employ a dimensionless form of the governing equations. To this end, we reduce Eq. (1) and Eq. (2) to dimensionless form by rescaling:

$$x\to\frac{m(g_1g_2)^{1/2}}{\hbar^2}x,\ t\to\frac{mg_1g_2}{\hbar^3}t,$$

$$V\to\frac{\hbar^2}{mg_1g_2}V,\ \psi_{1,2}\to\frac{\hbar}{m^{1/2}(g_1g_2)^{1/4}}\psi_{1,2}$$

$$
\begin{aligned}
i\partial_t\psi_1 &= -\frac{1}{2}\partial_x^2\psi_1 - V(x)\psi_1 \\
&+ G_1'|\psi_1|^2\psi_1 - G_{12}'|\psi_2|^2\psi_1 \\
&- \frac{1}{\pi}\left(\frac{g_1}{g_2}\right)^{1/4}\left(\frac{g_1}{g_2}|\psi_1|^2 + |\psi_2|^2\right)^{1/2}\psi_1,
\end{aligned} \tag{3}
$$

$$
\begin{aligned}
i\partial_t\psi_2 &= -\frac{1}{2}\partial_x^2\psi_2 - V(x)\psi_2 \\
&+ G_2'|\psi_2|^2\psi_2 - G_{12}'|\psi_1|^2\psi_2 \\
&- \frac{1}{\pi}\left(\frac{g_2}{g_1}\right)^{1/4}\left(\frac{g_2}{g_1}|\psi_2|^2 + |\psi_1|^2\right)^{1/2}\psi_2,
\end{aligned} \tag{4}
$$

with the dimensionless coefficients:

$$
G_1' = \sqrt{\frac{g_1}{g_2}} + \frac{2g_2\left(g_{12} + \sqrt{g_1 g_2}\right)}{(g_1+g_2)^2},
$$

$$
G_2' = \sqrt{\frac{g_2}{g_1}} + \frac{2g_1\left(g_{12} + \sqrt{g_1 g_2}\right)}{(g_1+g_2)^2},
$$

$$
G_{12}' = \frac{g_1^2 + g_2^2 - 2g_{12}\sqrt{g_1 g_2}}{(g_1+g_2)^2}.
$$

The coupled GPEs in Eqs. (3) and (4) can describe the dynamics of quasi-1D binary BEC mixtures in the presence of quantum fluctuations for arbitrary parameter settings and generic trap potentials. However, basic features of quantum droplets can be elucidated from simplified models by considering symmetric interaction coefficients $g_1 = g_2 = g$, equal atom numbers of the components $N_1 = N_2 = N$, and in the absence of a trap potential $V(x) = 0$. In such a special case with $\psi_1 = \psi_2 = \psi$, the coupled system of Eqs. (3) and (4) reduces to a single equation:

$$
\begin{aligned}
i\psi_t &= -\frac{1}{2}\psi_{xx} + \left(\frac{\delta g}{g}\right)|\psi|^2\psi - \frac{\sqrt{2}}{\pi}|\psi|\psi, \\
\delta g &= g + g_{12}
\end{aligned} \tag{5}
$$

Note that the coefficients g and g_{12} have opposite signs, namely the intra-component interaction is repulsive ($g > 0$), while the inter-component interaction is attractive ($g_{12} < 0$). At positive values of the coefficient of cubic nonlinearity ($\delta g / g > 0$), Eq. (5) admits an exact analytic solution [12, 13, 19]:

$$
\psi(x,t) = \frac{Ae^{-i\mu t}}{1 + B\cosh(\sqrt{-2\mu}x)}, \tag{6}
$$

where

$$
A = \sqrt{n_0}\,\frac{\mu}{\mu_0}, \quad B = \sqrt{1 - \frac{\mu}{\mu_0}},
$$

$$
n_0 = \frac{8}{9\pi^2}\left(\frac{g}{\delta g}\right)^2, \quad \mu_0 = -\frac{4}{9\pi^2}\frac{g}{\delta g}.
$$

This solution exists for negative values of the chemical potential $\mu < 0$ and transforms to a plane wave at $\mu = \mu_0$ with density $n = n_0$.

When the mean-field interactions exactly balance each other ($\delta g = 0$), the repulsive cubic nonlinearity in Eq. (5) vanishes, and the equation admits a solitonic solution known as the *quantum bright soliton* [16, 20–22]:

$$
\begin{aligned}
\psi(x,t) &= -\frac{3\pi\mu}{2\sqrt{2}}\,\mathrm{sech}^2(\sqrt{-\mu/2}\,x)e^{-i\mu t}, \\
\mu &= -\left(\frac{2N^2}{9\pi^4}\right)^{1/3}.
\end{aligned} \tag{7}
$$

Theoretical studies of one-dimensional QDs reported so far mainly considered the above-mentioned symmetric case in the absence of an external potential. In the following sections, we develop a variational approach by taking into account the external potential and validating it by numerical integration of the governing GPE. Numerical simulations were performed using the Fast Fourier Transform procedure [23], employing 2048 Fourier modes over the integration domain x ∈ [-50, 50] with periodic boundary conditions. The spatial step was set to $\Delta x = 0.05$ and the time step to $\Delta t = 0.001$. The results were obtained, and the figures were prepared using Mathematica software.

3. Methods: Variational Approach for Quantum Droplets

In this research, the Variational Approximation (VA) method is used to investigate the behavior and interaction of quantum droplets with an external potential

barrier. The process is analyzed in two cases: static and dynamic states of the QDs. In the first step, we use the Lagrangian formalism to derive the ordinary differential equations for the variational parameters, whose solution yields the static waveform of the QD. Next, the approximate waveform obtained from the static variational method is compared with the result of direct numerical integration of the time-dependent GPE. If the agreement between the two approaches is sufficiently strong, then the results are deemed reliable. This step is essential when examining the dynamics of nonlinear waves and their scattering by external potentials using the variational approach.

The VA method is one of the key theoretical tools for investigating non-integrable soliton-bearing equations, dating back to its first application by Anderson in 1983 [24]. After being successfully utilized to describe nonlinear pulse propagation in optical fibers, the method was extended to other fields, including quantum gases [25]. The VA method describes the evolution of localized waves using time-dependent variational parameters such as amplitude, width, and center-of-mass position. The system of ordinary differential equations for these variational parameters is obtained from the effective Lagrangian, corresponding to the original nonlinear Schrödinger-type equation. The main advantage of the VA method is that it allows for the description of both the static and dynamic properties of localized waves using a limited number of parameters. It can also predict the frequencies of internal vibrations in a perturbed soliton. Additionally, solving the system of ordinary differential equations is less computationally intensive than solving the original nonlinear partial differential equation.

The success of this method depends on choosing the right trial function to substitute into the Lagrangian density for further analysis. In our case, we have used a super-Gaussian function as an ansatz. The key factor here is that the trial function allows analytical evaluation of the spatial integrals to derive the effective Lagrangian.

4. Results and Discussion

The density profile of the QD depends on the number of atoms it contains. In the limit of a large number of atoms, the QD features a flat-top density profile [13], suggesting a super-Gaussian trial function for the variational analysis. The VA with a super-Gaussian ansatz in the context of nonlinear Schrödinger-type equations has been reported in several publications [26–30]. Below, we develop the static and dynamic VA for the GPE with cubic-quadratic nonlinearity in the presence of an external trap potential:

$$i\psi_t + \frac{1}{2}\psi_{xx} - V(x)\psi + g|\psi|^2\psi + q|\psi|\psi = 0, \tag{8}$$

where $\psi(x, t)$ is the wave function of the QD, and g and q are the coefficients of nonlinearity relevant to the residual mean-field and quantum fluctuations terms, respectively. The external potential is considered to be a harmonic trap $V(x) = \alpha x^2$. The dimensionless parameter $\alpha = (\omega_{\|}/\omega_{\perp})^2$ represents the trap aspect ratio and characterizes the strength (frequency) of the parabolic trap in the axial direction ($\omega_{\|}$) compared to the radial direction ($\omega_{\perp}$). The quasi-1D GPE (8) assumes that the transverse confinement is much stronger than the longitudinal one ($\omega_{\perp} \gg \omega_{\|}$) so that the radial dynamics is "frozen". The validity of VA is linked to the condition $\alpha \ll 1$. In the experiment reported in reference [31], the number of atoms was ~$2\cdot10^4$ and trap frequencies were $\omega_{\perp} = 2\pi \times 710$ Hz and $\omega = 2\pi \times 50$ Hz, which corresponds to $\alpha = 0.005$. In our numerical simulations, we set N = 15 (corresponding to ~10^4 atoms) and $\alpha = 0.001$. First, we find the stationary wave profile of the QD using the static version of the VA.

A. Static Variational Approximation

The stationary states of Eq. (8), which are looked for as $\psi(x, t) = \phi(x)\, exp(-i\mu t)$, satisfy the following equation:

$$\mu\phi + \frac{1}{2}\phi_{xx} - V(x)\phi + g\phi^3 + q\phi^2 = 0, \tag{9}$$

where μ is the chemical potential. The Lagrangian density generating this equation is

$$\mathcal{L} = \frac{1}{4}\phi_x^2 - \frac{\mu}{2}\phi^2 + \frac{1}{2}V(x)\phi^2 - \frac{g}{4}\phi^4 - \frac{q}{3}\phi^3. \tag{10}$$

The following super-Gaussian ansatz will be appropriate for the shape of a flat-top QD:

$$\phi(x) = A\exp\left[-\frac{1}{2}\left(\frac{x}{a}\right)^{2m}\right],$$
$$N = \int_{-\infty}^{+\infty}|\phi(x)|^2\,dx = 2A^2a\Gamma(1+M), \qquad (11)$$
$$M = \frac{1}{2m}.$$

where $\Gamma(z)$ is the gamma function [32], m is the super-Gaussian parameter, which can be a fractional number; thus, the exponential is understood as $exp(-(x/a)^{2m}) = exp(-(x^2/a^2)^m)$. The norm N of the trial function is expressed through the variational parameters: A is the amplitude, a is the width, and M is the reduced super-Gaussian parameter, as shown in Eq. (11). Using this ansatz, we get the averaged Lagrangian $L = \int \mathcal{L}dx$:

$$L = \frac{A^2\Gamma(2-M)}{8Ma} - \frac{gA^2a\Gamma(1+M)}{2^{M+1}} - \frac{qA^3a\Gamma(1+m)2^{M+1}}{3^{M+1}} - \mu A^2a\Gamma(1+M) + \alpha A^2a^3M\Gamma(3M). \qquad (12)$$

The VA equations are derived using the conditions $\partial L/\partial A = 0$, $\partial L/\partial a = 0$, $\partial L/\partial M = 0$. The chemical potential is obtained in the following form:

$$\mu = -\frac{3gN}{2^{M+3}a\Gamma(1+M)} - \frac{5qN^{1/2}2^{M-3/2}}{3^{M+1}\left[a\Gamma(1+M)\right]^{1/2}} + \frac{2\alpha a^2\Gamma(3M)}{\Gamma(M)}. \qquad (13)$$

The above three conditions together with the normalization of Eq. (11) are sufficient to obtain all four parameters A, a, m, μ. Figure 1 illustrates the stationary waveforms of the QD in free space ($\alpha = 0$) and in a harmonic trap ($a \neq 0$) derived from the static VA, and Figure 2 represents the time evolution of the waveforms according to the GPE.

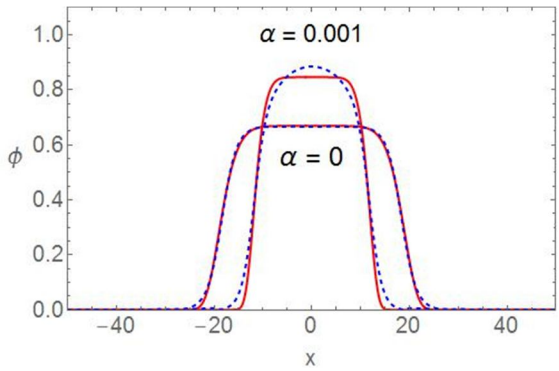

FIG. 1. The stationary wave profiles of a QD according to VA (red solid lines) and numerically obtained from GPE (blue dashed lines) in free space ($\alpha = 0$) and in a harmonic trap ($\alpha = 0.001$).

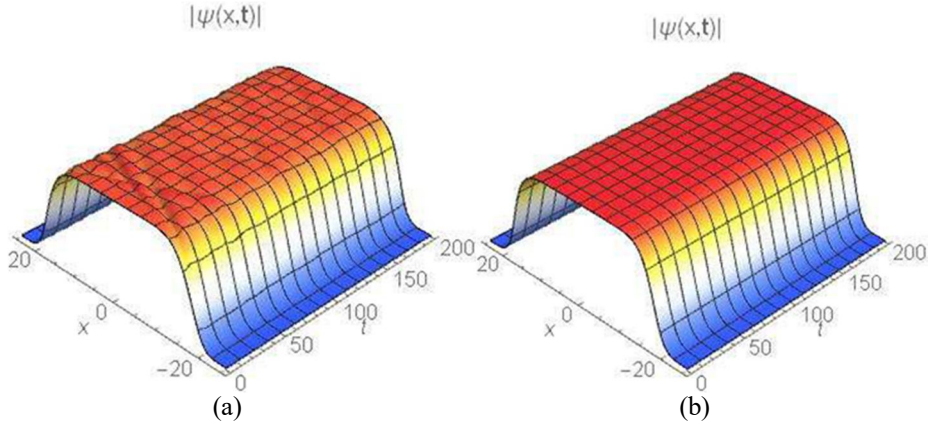

FIG. 2. (a) Numerical solution of Eq. (8) with initial waveform predicted by VA for $\alpha = 0$, (b) A similar result with exact initial waveform obtained from GPE using Nijhof's method [33].

As anticipated from Fig. 1, the trap causes the quantum droplet to squeeze, leading to a deviation from the flat-top shape in the central region. Here, the values of the parameters used were $N=15$, $A=0.669$, $a=17.774$, $m=4.116$, $g=-1$, $q=1$. The wave profiles of the QD predicted by VA and those calculated using the GPE show a greater divergence as the axial confinement increases, because under a stronger parabolic trap the QD becomes more compressed, changing its density profile from a flat-top to an inverted parabola. A good qualitative agreement between the numerically constructed and VA-predicted waveforms is evidence of the high accuracy of the VA approach applied to QDs. The time evolution of the VA-predicted waveform is verified by direct numerical simulations of Eq. (8), as shown in Fig. 2(a). Weak ripples on top of the QD are due to the approximate character of the variational method. Meanwhile, Fig. 2(b) shows the GPE simulation with the initial waveform obtained by Nijhof's method [33] where a completely stable propagation takes place for the numerically constructed exact initial waveform.

B. Dynamic Variational Approximation

Small-amplitude oscillations of a perturbed QD confined to a harmonic trap can be studied using the dynamic version of the variational approach, which we develop in this section. The Lagrangian density generating Eq. (8) is:

$$\mathcal{L}=\frac{i}{2}\left(\psi\psi_t^*-\psi^*\psi_t\right)+\frac{1}{2}\left|\psi_x\right|^2 +V(x)\left|\psi\right|^2-\frac{g}{2}\left|\psi\right|^4-\frac{2q}{3}\left|\psi\right|^3 . \quad (14)$$

To develop the dynamic version of the variational approach, we employ the super-Gaussian trial function:

$$\psi(x,t)=A\exp\left[-\frac{1}{2}\left(\frac{x}{a}\right)^{2m}+ibx^2+i\varphi\right], \quad (15)$$

where $A(t)$, $a(t)$, $b(t)$ and $\varphi(t)$ are the time-dependent variational parameters, denoting the amplitude, width, chirp and phase of the flat-top QD, respectively. The super-Gaussian parameter m is obtained from the static VA, and we assume it is known. The wave function is normalized to the reduced number of atoms in the droplet:

$$N=\int_{-\infty}^{+\infty}\left|\phi(x)\right|^2dx=2A^2a\Gamma(1+M), \quad M=\frac{1}{2m}, \quad (16)$$

with $\Gamma(z)$ being the gamma function [29]. Then, the averaged Lagrangian $L=\int\mathcal{L}dx$ computed with the trial function expressed by Eq. (15) is obtained:

$$\frac{L}{N}=\frac{\Gamma(3M)}{\Gamma(M)}\left(a^2b_t+2a^2b^2+\alpha a^2\right) +\frac{\Gamma(2-M)}{8M^2\Gamma(M)a^2}-\frac{gN}{2^{M+2}M\Gamma(M)a} -\frac{2^{M+1/2}}{3^{M+1}}\cdot\frac{qN^{1/2}}{\left(M\Gamma(M)\right)^{1/2}a^{1/2}}+\varphi_t. \quad (17)$$

From this Lagrangian we get the equation for the variational parameter a:

$$a_{tt}=\frac{\Gamma(2-M)}{4M^2\Gamma(3M)a^3}-\frac{gN}{2^{M+2}M\Gamma(3M)a^2} -\frac{2^{M-1/2}}{3^{M+1}}\cdot\frac{qN^{1/2}\Gamma(M)^{1/2}}{M^{1/2}\Gamma(3M)a^{3/2}}-2\alpha a. \quad (18)$$

The last equation is formally similar to the equation of motion of a unit mass particle in an effective potential $a_{tt}=-\partial U/\partial a$. The corresponding potential is found by integration of the right-hand side of Eq. (18):

$$U(a)=\frac{\Gamma(2-M)}{8M^2\Gamma(3M)a^2}-\frac{gN}{2^{M+2}M\Gamma(3M)a} -\frac{2^{M+1/2}}{3^{M+1}}\cdot\frac{qN^{1/2}\Gamma(M)^{1/2}}{M^{1/2}\Gamma(3M)a^{1/2}}+\alpha\cdot a^2 . \quad (19)$$

The effective potential given by Eq. (19) for two different values of the harmonic trap strength $V(x)=\alpha x^2$ is shown in Fig. 3(a). The position of the minimum of this potential gives the stationary width of the QD through the fixed point of Eq. (18).

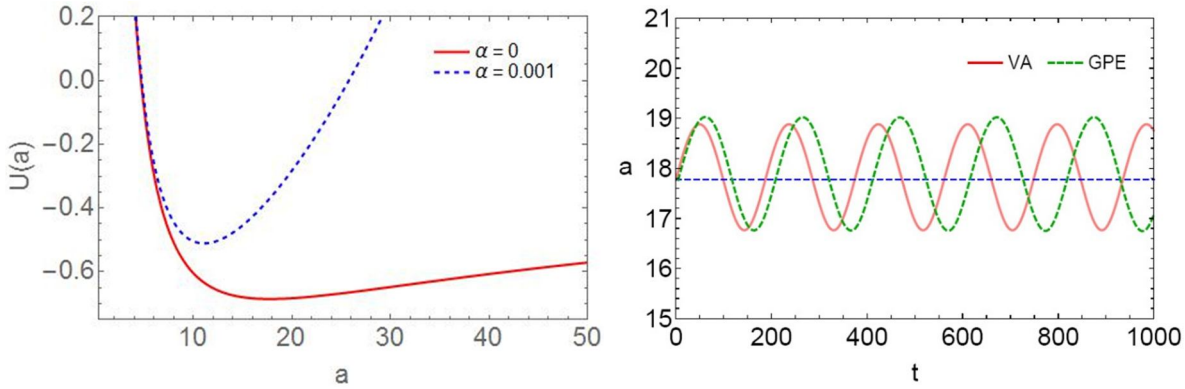

(a) (b)

FIG. 3. (a) The effective potential $U(a)$ given by Eq. (19) for different strengths of the harmonic trap $V(x)=\alpha x^2$ (b) The evolution of the parameter a(t) according to the VA expressed by Eq. (18) (red solid line) and GPE (given by Eq. 8) (green dashed line).

As can be seen from this figure, in the absence of the trap potential, the QD is wide, while in the presence of the harmonic trap, it shrinks notably from $a_0=17.774$ to $a_0=11.1$.

To compare the predictions of the VA with the results of the numerical solution of the GPE given by Eq. (8), the relation between the mean square width of the QD, as defined by Eq. (20) and the variational parameter *a(t)* has to be established:

$$w^2(t)=\frac{1}{N}\int_{-\infty}^{\infty}x^2\left|\psi(x,t)\right|^2dx, \qquad (20)$$

Substitution of the trial function given by Eq. (15) into Eq. (20) yields the required relation:

$$w(t)=a(t)\sqrt{\left(\Gamma(3M)/\Gamma(M)\right)}.$$

In Fig. 3(b), the evolution of the parameter *a*(t) according to the VA as given by Eq. (18) is shown along with the corresponding results of the GPE simulations: $a_{GPE}(t)=w(t)\sqrt{\left(\Gamma(M)/\Gamma(3M)\right)}$.

It can be seen that the width of the perturbed QD oscillates (red solid line) near the stationary point (blue dashed line) with the frequency predicted by the VA to be:

$$\omega_0=(\partial^2U/\partial a^2\,|_{(a=a_0)})^{1/2}\approx 0.033.$$

The initial conditions established using the VA are: $a(0)=a_0$, $\dot{a}(0)=2a_0b_0$, $a_0=17.774$, $b_0=0.001$, $M=0.1214$ and $\alpha=0$.

The green dashed line corresponds to the evolution of the wave profile given by Eq. (15) with the parameters:

$$A=0.669,\ a=a_0,\ b=b_0,\ m=4.116,\ \varphi=0$$

according to the GPE given by Eq. (8) for g = –1, q = 1, and $\alpha=0$. It should be emphasized that in numerical GPE simulations, we use the wave profile and chirp parameter predicted by VA. The approximate nature of the VA results in greater oscillation amplitudes and an increasing phase shift with time, as observed in Fig. 3(b).

C. Reflection From a Potential Barrier

Although quantum droplets are extremely dilute compared to ordinary liquids, they display liquid-like behavior during mutual collisions [34] and scattering from external potentials. In the numerical experiment, we consider a QD comprising a large number of atoms, thus featuring a flat-top wave profile. The droplet is confined to a weak harmonic trap with a sufficiently high and narrow potential barrier at its center. The initial position of the droplet is shifted from the center of the harmonic trap, so that it starts to move under the action of the potential. A typical process of interaction of a QD with a potential barrier is illustrated in Fig. 4.

As shown, the QD reflects off the potential barrier like a liquid droplet bouncing off a nonwetting wall. The reflection of the quantum droplet from the potential barrier exhibits clear liquid-like behavior. Interference phenomena, associated with the reflection of wave packets from potential barriers, are suppressed. The tunnelling process (leakage of matter to another

side of the barrier) is also absent, which may be linked to the effect of QD's surface tension. The phenomena related to the interaction of QDs with potential barriers and wells can provide valuable information about their incompressibility and surface tension.

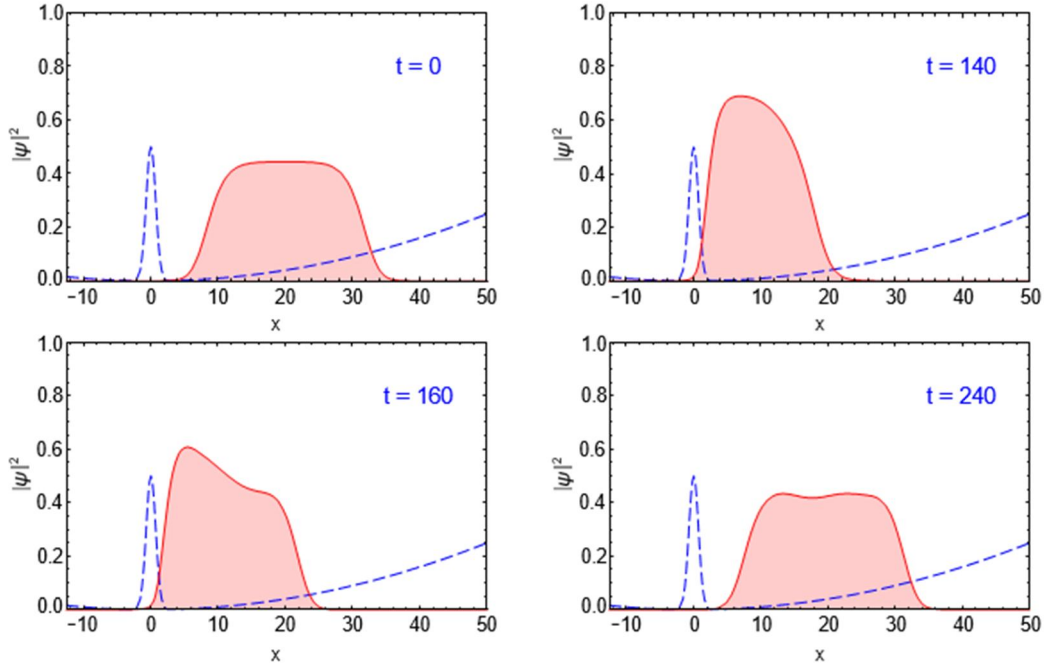

FIG. 4. Motion of a quantum droplet in a weak harmonic potential with a barrier at the center $V(x) = 5 \cdot 10^{-5}x^2 + 0.5\exp(-x^2)$, illustrated for several time instances from t = 0 to t = 240.

5. Conclusion

The properties of quasi-one-dimensional quantum droplets governed by the GPE with competing cubic-quadratic nonlinearity have been studied using analytical and numerical methods. For the symmetric parameter setting with equal strength of intra-species repulsion and an equal number of atoms in both components of the binary Bose-Einstein condensate, a variational approach has been developed. Comparison of the analytical predictions with the numerical simulations of the GPE showed good qualitative agreement, suggesting that the super-Gaussian trial function can successfully describe the peculiar flat-top shape of the QD's wave function. In numerical experiments, a liquid-like reflection of QDs from the potential barrier has been observed. The insights obtained from this study open up several promising future research directions. In particular, the findings can stimulate new experiments with ultra-dilute quantum liquids and lead to further progress in the development of devices for quantum technologies [35]. A relevant topic is the existence and properties of quantum droplets with unequal numbers of atoms, masses, and interaction strengths among the components [36]. These studies can shed new light on the limits of QD stability against violation of presumed symmetries.

Acknowledgements

This research was supported by a grant from the Ministry of Higher Education of Malaysia for the International Islamic University of Malaysia, project code FRGS/1/2021/STG06/UIAM/03/1 with project ID: FRGS21-232-0841. BBB thanks the Faculty of Science at IIUM, Malaysia, for their hospitality during his visit.

References

[1] Luo, Z.H., Pang, W., Liu, B., Li, Y., and Malomed, B.A., Front. Phys., 16 (2021) 32201.

[2] Guo, M. and Pfau, T., Front. Phys., 16 (2021) 32202.

[3] Malomed, B.A., "Multidimensional Solitons", (AIP Publishing, Melville, New York, 2022).

[4] Petrov, D.S., Phys. Rev. Lett., 115 (2015) 155302.

[5] Kadau, H., Schmitt, M., Wenzel, M., Wink, C., Maier, T., Ferrier-Barbut, I., and Pfau, T., Nature, 530 (2016) 194.

[6] Ferrier-Barbut, I., Kadau, H., Schmitt, M., Wenzel, M., and Pfau, T., Phys. Rev. Lett., 116 (2016) 215301.

[7] Cabrera, C., Tanzi, L., Sanz, J., Naylor, B., Thomas, Cheiney, P., and Tarruell, L., Science, 359 (2018) 301.

[8] Semeghini, G., Ferioli, G., Masi, L., Mazzinghi, C., Wolswijk, L., Minardi, F., Modugno, M., Modugno, G., Inguscio, M., and Fattori, M., Phys. Rev. Lett., 120 (2018) 235301.

[9] Lee, T.D., Huang, K., and Yang, C.N., Phys. Rev., 106 (1957) 1135.

[10] Lieb, E.H. and Liniger, W., Phys. Rev., 130 (1963) 1605.

[11] Edler, D., Mishra, C., WÄachtler, F., Nath, R., Sinha, S., and Santos, L., Phys. Rev. Lett., 119 (2017) 050403.

[12] Petrov, D.S. and Astrakharchik, G.E., Phys. Rev. Lett., 117 (2016) 100401.

[13] Astrakharchik, G.E. and Malomed, B.A., Phys. Rev. A, 98 (2018) 013631.

[14] Pethick, C.J. and Smith, H., "Bose-Einstein condensation in dilute gases", (Cambridge University Press, 2008).

[15] Petrov, D.S., Nature Physics, 14 (2018) 211.

[16] Otajonov, Sh.R., Tsoy, E.N., and Abdullaev, F.Kh., Phys. Lett. A, 383 (2019) 125980.

[17] Nikolaou, S., Kavoulakis, G.M., and Ogren, M., Phys. Rev. A, 110 (2024) 043302.

[18] Mithun, T., Maluckov, A., Kasamatsu, K., Malomed, B.A., and Khare, A., Symmetry, 12 (2020) 174.

[19] Triki, H., Biswas, A., Moshokoa, S.P., and Belic, M., Optik, 128 (2017) 63.

[20] Liu, B., Zhang, H.-F., Zhong, R.-X., Zhang, X.-L., Qin, X.-Z., Huang, C., Li, Y.-Y., and Malomed, B.A., Phys. Rev. A, 99 (2019) 053602.

[21] Tononi, A., Wang, Y., and Salasnich, L., Phys. Rev. A, 99 (2019) 063618.

[22] Gangwar, S., Ravisankar, R., Muruganandam P., and Mishra, P.K., Phys. Rev. A, 106 (2022) 063315.

[23] Agrawal, G.P., "Nonlinear Fiber Optics", (Academic Press, San Diego, CA, 1989).

[24] Anderson, D., Phys. Rev. A, 27 (1983) 1393.

[25] Malomed, B.A., "Variational Methods in Nonlinear Fiber Optics and Related Fields", Ed. E. Wolf, "Progress in Optics", Vol. 43 (North-Holland, Amsterdam, 2002), pp. 69 - 191.

[26] Karlsson, M., Phys. Rev. A, 46 (1992) 2726.

[27] Tsoy, E.N., Ankiewicz, A., and Akhmediev, N., Phys. Rev. E, 73 (2006) 036621.

[28] Baizakov, B.B., Bouketir, A., Messikh, A., Benseghir, A., and Umarov, B.A., Int. J. Mod. Phys. B, 25 (2011) 2427.

[29] Umarov, B.A., Aklan, N.A.B., Rosly, M.R., and Hassan, T.H., J. Phys.: Conf. Ser., 890 (2017) 012071.

[30] Umarov, B.A. and Aklan, N.A.B., J. Phys.: Conf. Ser., 819 (2017) 012023.

[31] Khaykovich, L., Schreck, F., Ferrari, G., Bourdel, T., Cubizolles, J., Carr, L.D., Castin, Y., and Salomon, C., Science, 296 (2002) 1290.

[32] Abramowitz, M. and Stegun, I.A., "Handbook of Mathematical Functions", (National Bureau of Standards, Washington, 1964).

[33] Nijhof, J.H.B., Forysiak, W., and Doran, N.J., IEEE J. Sel. Top. Quantum Electron., 6 (2000) 330.

[34] Ferioli, G., Semeghini, G., Masi, L., Giusti, G., Modugno, G., Inguscio, M., Gallemi, A., Recati, A., and Fattori, M., Phys. Rev. Lett., 122 (2019) 090401.

[35] Amico, L., Anderson, D., Boshier, M., Brantut, J.P., Kwek, L.C., and Minguzzi, A., Rev. Mod. Phys., 94 (2022) 041001.

[36] Englezos, I.A., Schmelcher, P., and Mistakidis, S.I., Phys. Rev. A, 110 (2024) 023324.